Biochimica et Biophysica Acta, 1099 (1992) 163–169

BBABIO 43561

Independent fluorescence emission of the chlorophyll spectral forms in higher plant Photosystem II

Giuseppe Zucchelli, Robert C. Jennings and Flavio M. Garlaschi

Centro C.N.R. Biologia Cellulare e Molecolare delle Piante, Dipartimento di Biologia, Università di Milano, Milano (Italy)

(Received 12 July 1991)

Key words: Fluorescence emission; Numerical deconvolution; Chlorophyll spectral forms; Light-harvesting chlorophyll *a*/*b* protein complex II; (Spinach and barley thylakoids)

Room-temperature steady-state emission and Q_y absorption spectra of light-harvesting chlorophyll *a*/*b* protein complex II (LHCII) isolated from spinach have been analysed in terms of a linear combination of asymmetric gaussian bands. To investigate a possible correspondence between the absorption and emission bands, the thermal emission spectrum of each absorption band has been calculated. It is demonstrated that the calculated fluorescence bands correspond closely to those obtained by gaussian deconvolution. It is thus possible to associate an emission band with each absorbing chlorophyll spectral species: Chl_{653}^{648}, Chl_{663}^{661}, Chl_{672}^{670}, Chl_{680}^{678}, Chl_{687}^{684}, Chl_{697}^{695} (Chl_m^n is the spectral species that absorbs with maximum at wavelength *n* and emits with maximum at wavelength *m*) and to interpret the emission spectrum of LHCII as a linear combination of the emission spectra of each absorbing chlorophyll spectral species. In particular, the correspondence between the 684 nm and 695 nm absorption bands and the emission bands with maximum at 687 nm and 697 nm lends support to the presence of long wavelength Chl *a* spectra forms in LHCII, the external antenna of PS II. A close correlation between the emission and absorption gaussian bands is also found in the analysis of the room temperature absorption and emission spectra of such membrane preparation as BBY-grana from spinach and thylakoids prepared from barley wild type and the chlorina f2 mutant (lacking LHCII). On the basis of these data, the commonly observed 5–7 nm wavelength difference between the absorption and emission spectra maxima of chlorophyll containing biological membranes is interpreted in terms of (a) the Stokes shifts of the single spectral forms together with (b) the increased emission contribution of the longer wavelength forms to the emission spectrum caused by energy transfer.

Introduction

The photosystems of green plants absorb light by means of a large array of chromophores, mainly chlorophylls, bound to specific polypeptides to form chlorophyll-protein complexes [1,2]. The number of antenna chlorophylls per reaction centre is dependent on the type of plant and growth conditions. In normally grown plants there are, on average, about 200–250 antenna Chls per RC [3,4].

The antenna array is formed by two distinct Chl species, *a* and *b*, with greater amounts of Chl *a*. Chlorophyll *a* is thought to be present as different spectral forms, each with a different absorption maximum [5]. This spreading of the spectral properties of Chl *a* is probably caused by environmental perturbations of the electronic transition due to local effects [6]. The interpretation of the absorption spectra of photosynthetic membranes in terms of different spectral forms relies mainly on derivative spectroscopy and sub-bands numerical deconvolution of the Q_y region of the absorption spectra in terms of gaussian or lorentzian components [5,7–12].

The spectral heterogeneity of the chloroplast absorption spectrum raises the question as to whether the fluorescence emission spectrum might not also be heterogeneous with each of the absorption spectral forms having a distinct emission. Emission heterogeneity at low temperature is well known [9,11,13,14] but is not

Abbreviations: BBY-grana, Berthold, Babcock, Yocum [24]; Chl, chlorophyll; DCMU, 3-(3,4-dichlorophenyl)-1,1-dimethylurea; DBMIB, dibromothymoquinone; F_m, fluorescence yield with reaction centres closed; F_0, fluorescence yield with reaction centres open; F_v, fluorescence at the plateau level of the fast induction phase; fwhm, full width at half maximum; LHCII, light harvesting chlorophyll *a*/*b* protein complex II; PSI, Photosystem I; PS II, Photosystem II; RC, reaction centre; Tricine, *N*-tris(hydroxymethyl)methylglycine.

Correspondence: G. Zucchelli, Centro C.N.R. Biologia Cellulare e Molecolare delle Piante, Dipartimento di Biologia, Università di Milano, via Celoria 26, 20133 Milano, Italy.

thought to be associated with the individual absorption spectral forms. Marchiarullo and Ross [15], working with room-temperature chloroplast emission spectra, which were analysed by factor analysis, demonstrated only a limited (two components) heterogeneity which they associated with the photosystems. We have recently demonstrated [16,17] on the basis of a careful analysis of the chloroplast fluorescence excitation and emission spectra that the quenching of PS II fluorescence is a function of both excitation and emission wavelength. These RC-fluorescence excitation and emission quenching spectra are readily interpreted in terms of a separate fluorescence emission by each of the chlorophyll spectral forms. In the present paper this aspect is further investigated.

The long wavelength absorption and emission spectra of a complex molecule can be connected by a 'universal' relationship, determined on thermodynamic grounds, which is based on the attainment of thermal equilibrium between the vibrational degrees of freedom both of the ground and the emitting electronic states of the molecule [18]. This relationship, the experimental validity of which has been checked for a variety of molecules in solution and also in semiconductors [19,20], has been used here to investigate whether the emission spectrum of a photosynthetic membrane may be represented as a linear combination of different Chl spectral emission forms. We have initially analysed the correlations between the absorption and the emission bands obtained by gaussian deconvolution of the LHCII room-temperature absorption and emission spectra. Subsequently this analysis has been extended to membrane preparations such as spinach BBY-grana and chloroplasts from barley wild type and chlorina f2 mutant (lacking LHCII).

Materials and Methods

LHCII was prepared from spinach leaves according to Ryrie et al. [21] using Triton X-100 as detergent. Final resuspension was in a medium containing sucrose (0.05 M) and Tricine (5 mM, pH 8). The Chl *a* to Chl *b* ratio was 1.1 measured according to Arnon [22]. In these conditions our LHCII preparation is thought to be in the microcrystalline lamellar sheet form of LHCII [23].

BBY-grana (enriched in PS II) were prepared from freshly harvested spinach leaves according to Berthold et al. [24] with omission of the last Triton X-100 treatment [11]. This preparation contains both LHCII and the PS II core protein complexes and is substantially free of PS I chlorophyll-protein complexes (data not shown).

Thylakoids from barley wild type and the chlorina f2 mutant were prepared from freshly harvested leaves as previously described [25] and resuspended in Tricine (30 mM; pH 8), NaCl (10 mM), $MgCl_2$ (5 mM) and sucrose (0.2 M).

Absorption and emission spectra were measured using an EG&G OMAIII (model1460) with an intensified diode array (model 1420) mounted on a spectrograph (Jobin-Yvon HR320) with a 150 groove mm^{-1} grating. The wavelength scale of the instrument was calibrated using a neon spectral calibration source (Cathodeon). The wavelength spacing between pixels is about 0.5 nm. An OG 530 filter (Schott) was placed before the collection optics to diminish stray light.

The absorption spectra were measured using a 1 mm pathlength cuvette with an opal glass placed behind to substantially eliminate scattering artifacts [26]. The residual absorption around 750 nm has been subtracted from the spectra when present (BBY-grana and thylakoids). The chlorophyll concentration was about 10 μg/ml, giving a maximum Q_y absorbance of about $25 \cdot 10^{-3}$. Each spectrum is the sum of $3 \cdot 10^4$ scans. The incident white light from an halogen lamp was attenuated by neutral filters.

The emission spectra were measured using transmission geometry. The samples utilised were the same as for the absorption measurement but without opal glass. DCMU (25 μM) was added to BBY-grana and thylakoids samples to reach the maximum fluorescence level. The exciting light was filtered through a combination of a 4-96 filter (Corning) and a 450 nm interference filter (Oriel) with a 10 nm bandpass. The background reading was measured in the presence of the fluorescence quencher DBMIB (280 μM), which eliminates over 99% of the peak fluorescence, and then subtracted from the measured spectrum. The maximum number of counts in each spectrum was of the order of $2 \cdot 10^5$. The emission spectra were corrected for distortions resulting from a wavelength dependent response of the light collection setup using an intensity calibrated source (ISCO Spectroradiometer Calibrator).

The emission spectra with open and closed RCs were measured using a 10 mm pathlength cuvette and the apparatus described above but with some modifications: excitation light was provided by an Heath monochromator (excitation wavelength 430 nm, fwhm 1.2 nm) combined with two Corning 4-96 filters and the viewing angle was 90° with respect to the exciting light. In this way the level of stray light was not significant at wavelengths above 650 nm, as judged by using DBMIB. Each spectrum is the sum of 40 scans with a maximum number of counts around 12000 in each scan at the F_m level. Fluorescence was maintained near the F_0 level (open RCs; F_i) by means of a weak excitation beam and continual sample stirring in the presence of methylviologen (0.1 mM). Only a small part of the sample was illuminated. Emission spectra with closed RCs (F_m) were measured after the addition of 25 μM DCMU and 2 mM hydroxylamine.

Deconvolution analyses of the spectra in terms of 'asymmetric' gaussian bands were performed as already described [12]. The absorption and emission spectra were analysed independently to find the minimal number of bands giving the best fit, as judged using the χ^2 and the distribution of the residuals [27]. All the band parameters were left free in the fitting of both the absorption and emission spectra.

Results

Room temperature absorption and emission spectra of LHCII, the external antenna of PS II, are shown in Fig. 1 with the gaussian bands obtained by numerical deconvolution. The band parameters are reported in Table I. The wavelength spacing between the two spectral maxima is about 5 nm. The absorption spectrum is resolved into the usually observed bands [5,7–12] i.e., the Chl *b* band at about 648 nm, the four major Chl *a* bands up to 684 nm and two minor forms at longer wavelengths. The fluorescence emission spectrum is described as the sum of two main emission bands with maxima at about 680 nm and 687 nm and of nearly equal area and several minor bands both at shorter and at longer wavelengths.

As indicated above, the absorption bands are normally interpreted as the electronic band of different chlorophyll spectral species. If it is assumed that thermal equilibrium between the vibrational degrees of freedom of each excited species is reached before emission, one may calculate from each absorption band the expected emission band at a given temperature, using the Stepanov [18] relation

$$\frac{F(\nu)}{A(\nu)\nu^3} = C\, e^{-\frac{h}{k_B T}(\nu - \nu_{el})} \qquad (1)$$

where $A(\nu)$ is the absorption spectrum, $F(\nu)$ is the emission spectrum, C is a constant, k_B is the Boltzmann constant, T is the absolute temperature of the surrounding medium, h is the Planck constant and ν_{el}, using the terminology of Stepanov, is the frequency of the purely electronic transition, a constant for each band.

In Fig. 2 the comparison between the emission bands calculated from the absorption bands with maxima between 648 nm and 695 nm and the emission bands obtained by deconvolution of the emission spectrum up to the 697 nm band is shown. It should be emphasised that the fluorescence yield does not explicitly appear in the Stepanov expression, Eqn. 1. For this reason the calculated emission bands have been normalised to the height of the corresponding fluorescence bands obtained by numerical deconvolution. It is evident that there is a rather close correspondence between the calculated emission bands and those determined by the

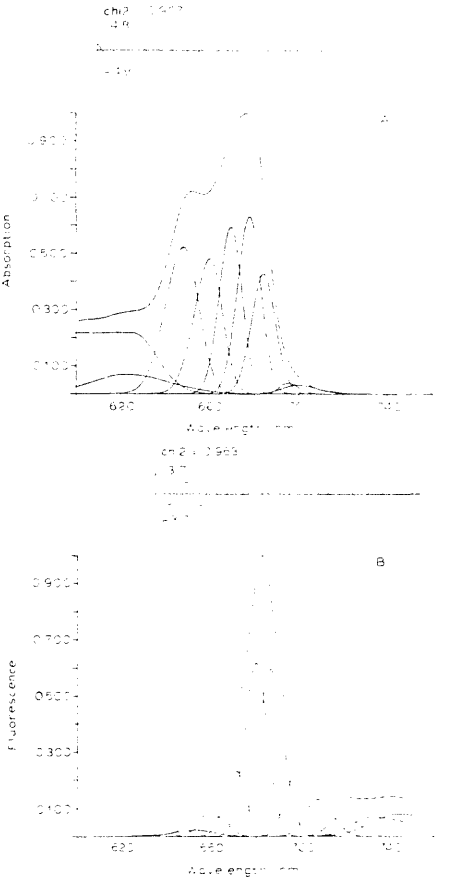

Fig. 1. Room temperature absorption and emission spectra of LHCII with the relative gaussian bands obtained by numerical analysis. The band parameters are given in Table I. The emission spectrum has been corrected for the sensitivity of the measuring apparatus (see Materials and Methods). The spectra have been normalized to the peak value. Plots of the residuals are also shown.

emission spectrum deconvolution. Thus, it is possible to associate an emission band with each absorbing Chl spectral species: Chl_{653}^{18}, Chl_{663}^{660}, Chl_{672}^{670}, Chl_{680}^{678}, Chl_{687}^{684}, Chl_{697}^{695} (Chl_m^n is the spectral species that absorbs with maximum at wavelength n and emits with maximum at wavelength m). The relative contribution of the fluorescence bands to the emission spectrum is rather similar to that expected on the basis of a Boltzmann-weighted band population distribution between the

TABLE I

Gaussian parameters for the deconvolution of the room-temperature absorption (A) and emission (F) spectra of spinach LHCII and a spinach grana preparation (BBY-grana)

The percentage area has been calculated from the sum of all the bands in the Table. The fwhm is given as a left and right value. The fwhm of each band is the sum of the two values. The parameters for the shorter wavelength bands obtained by gaussian deconvolution of the absorption spectra as well as the longest wavelength bands obtained in the deconvolution of the emission spectra are not shown. All the band parameters were left free in these fits.

Band	LHCII		BBY-grana	
	A	*F*	*A*	*F*
1 λ_{max}	648.5	652.9	647.5	653.4
fwhm	9.6 7.9	11.0 10.2	9.4 7.5	10.6 10.2
Area %	24.48	2.20	17.51	1.99
2 λ_{max}	660.4	663.0	660.0	663.6
fwhm	8.2 6.5	8.6 5.7	8.3 7.3	8.7 8.4
Area %	19.01	4.72	19.97	4.82
3 λ_{max}	669.7	671.6	669.6	671.7
fwhm	6.1 5.6	6.1 4.8	6.4 5.6	6.7 5.2
Area %	18.70	11.82	21.32	15.59
4 λ_{max}	677.8	680.2	677.5	679.7
fwhm	6.2 6.0	6.0 5.9	5.4 5.4	5.6 5.3
Area %	20.67	34.34	21.42	35.80
5 λ_{max}	684.0	686.8	683.9	686.5
fwhm	6.3 6.5	6.2 6.6	5.4 6.7	5.7 7.4
Area %	14.63	35.48	12.97	32.54
6 λ_{max}	694.9	697.3	695.1	699.4
fwhm	4.1 5.8	5.4 6.4	4.6 9.2	5.6 7.7
Area %	1.01	11.45	2.56	9.26
7 λ_{max}	699.5		708.8	
fwhm	8.0 9.9		33.0 17.0	
Area %	1.50		4.24	

excited states of the different chromophores (see Table II).

The extensive overlapping between the long-wave-

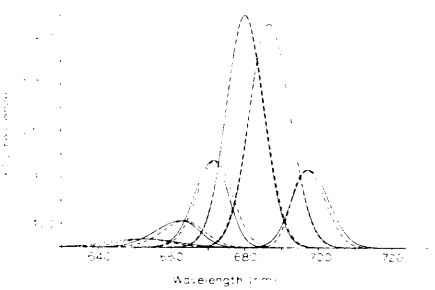

Fig. 2. Comparison between the fluorescence bands obtained by numerical deconvolution of the emission spectrum of LHCII and the emission bands calculated from the absorption bands. ———, emission bands obtained by numerical deconvolution; – – –, calculated emission bands. The emission bands calculated from the absorption bands using the Stepanov relationship (Eqn. 1) for a temperature $T = 300$ K are normalized to the height of the corresponding numerical emission bands.

TABLE II

The comparison between the percentage contribution of the different chlorophyll-emitting species to the emission spectrum of LHCII obtained by bands deconvolution and calculated using the Boltzmann distribution

The Boltzmann values have been calculated from the λ_{max} of the absorption bands of LHCII (see Table I) using the absorption band peaking at 694.9 nm as reference and the relative areas under the absorption bands as weighting factors. Temperature $T = 300$ K.

λ_{max}^{em} (nm)	652.9	663.0	671.6	680.2	686.8	697.3
Numerical deconvolution	2.20	4.72	11.82	34.34	35.48	11.45
Boltzmann factor	1.56	4.50	12.00	31.30	42.00	8.70

length absorption and the emission spectra of LHCII prompted us to formally use the Stepanov relation to calculate the total absorption spectrum from the emis-

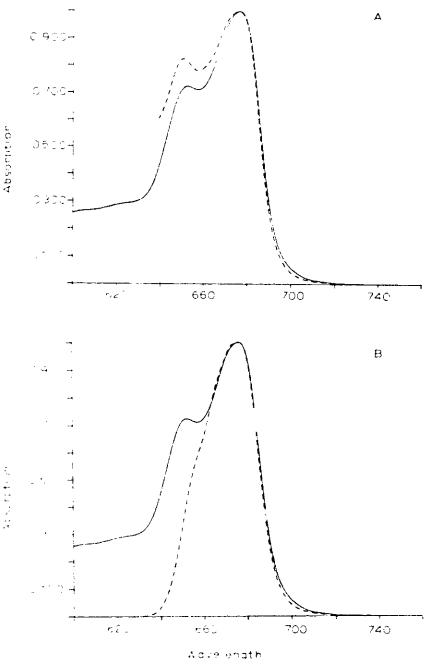

Fig. 3. Comparison between measured and calculated absorption spectra of LHCII. ———, experimental; – – –, calculated. (A) The calculated absorption spectrum has been obtained from the measured emission spectrum using the Stepanov relationship (Eqn. 1) for a temperature $T = 300$ K. (B) The calculated absorption spectrum has been obtained as in (A) but using the measured emission spectrum with the minor band peaking at about 653 nm deleted from it.

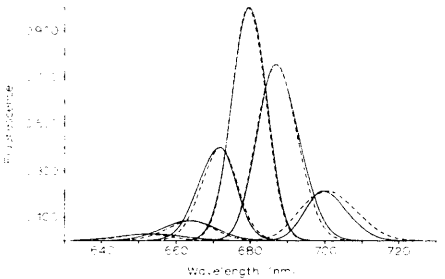

Fig. 4. Comparison between the fluorescence bands obtained by the numerical deconvolution of the BBY-grana emission spectrum and the emission bands calculated from the absorption bands. ———, emission bands obtained by numerical deconvolution; – – –, calculated emission bands. For other details see Fig. 2.

sion one. The result is shown in Fig. 3a where the calculated absorption spectrum for $T = 300$ K is compared with the measured absorption spectrum. It can be seen that the resemblance between calculated and measured absorption spectra is good, with also the Chl *b* absorption peak present. On the other hand, when

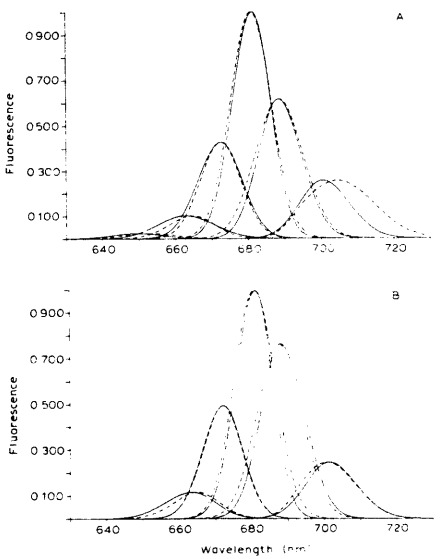

Fig. 5. Comparison between the fluorescence bands obtained by numerical deconvolution of the emission spectra of thylakoids from barley wild type (A) and the chlorina f2 mutant (B) and the emission bands calculated from the absorption bands. ———, emission bands obtained by numerical deconvolution; – – –, calculated emission bands. For other details see Fig. 2.

TABLE III

Gaussian parameters for the deconvolution of the room temperature absorption (A) and emission (F) spectra of thylakoids from barley wild type and the chlorina f2 mutant

For details see Table I.

Band	Barley W.T.		Chlorina mutant	
	A	*F*	*A*	*F*
1 λ_{max}	647.8	650.0	647.5	
fwhm	10.6 8.2	8.8 7.8	13.3 9.9	
Area %	17.24	1.17	9.66	
2 λ_{max}	660.6	662.7	661.9	663.6
fwhm	8.1 7.3	8.8 9.4	8.6 7.2	8.7 7.4
Area %	18.28	5.49	17.65	5.36
3 λ_{max}	669.3	672.5	669.3	672.2
fwhm	6.9 6.6	7.4 6.8	7.0 6.2	6.7 6.2
Area %	20.04	18.14	22.50	18.19
4 λ_{max}	677.7	681.1	677.6	681.0
fwhm	6.8 6.6	6.4 6.0	6.4 6.7	6.4 5.6
Area %	20.74	37.07	22.25	33.99
5 λ_{max}	684.3	688.2	684.0	688.0
fwhm	7.7 7.8	6.5 7.5	7.2 7.3	6.5 7.6
Area %	16.54	25.82	20.18	30.83
6 λ_{max}	695.7	700.4	695.1	701.3
fwhm	6.0 11.7	7.4 8.7	6.3 9.3	7.7 8.9
Area %	5.32	12.31	6.31	11.62
7 λ_{max}	714.2		709.5	
fwhm	11.1 16.4		5.9 13.1	
Area %	1.85		1.45	

the small band peaking at about 653 nm is subtracted from the measured emission spectrum and then the absorption spectrum is subsequently calculated, all traces of the Chl *b* absorption peak are absent (Fig. 3b). This observation suggests that the minor emission band peaking near 653 nm in the spectral deconvolution of the emission spectrum is due to Chl *b*. In this respect it should be noted that the 653 nm band corresponds closely to the expected Chl *b* fluorescence calculated using the Stepanov relation (Eqn. 1) (Fig. 2).

A similar analysis has also been performed for the absorption and emission spectra of the BBY-grana preparation. The parameters of the gaussian band deconvolution are reported in Table I. All the bands found in the absorption and emission spectra of LHCII are also present in the deconvolution of the absorption and emission spectra of BBY-grana.

We have calculated for BBY-grana the emission bands from the absorption ones using the Stepanov relation (Eqn. 1) for $T = 300$ K (Fig. 4). The absorption bands utilised ranged from 648 nm to 695 nm. The correspondence between the calculated emission bands and those obtained by the fitting procedure is good so that, also in this case, it is possible to associate an emission band with each absorbing chlorophyll spectral species.

As noted from the above analysis of LHCII, there is a minor emission band peaking at about 653 nm which

can be associated with Chl *b* using the Stepanov relation. When the overall BBY-grana absorption spectrum is calculated from the emission one, the spectrum obtained resembles the measured one with the presence of the Chl *b* absorption shoulder. On the other hand, if the minor emission band at 653 nm is deleted from the measured emission spectrum and then the absorption spectrum is calculated, the Chl *b* absorption shoulder disappears (data not shown), as found for LHCII.

The absorption and emission spectra of thylakoids from barley wild type and the chlorina mutant, lacking LHCII, have also been analysed by gaussian deconvolution. The parameters obtained are reported in Table III. The emission spectra utilised for this analysis are the spectra of the variable fluorescence $F_m - F_0$. In this way the fluorescence is expected to be substantially free of any PS I emission contribution. The comparison between the emission bands calculated from the absorption bands using the Stepanov relation (Eqn. 1) and the fluorescence bands obtained by gaussian deconvolution of the measured emission spectra is shown in Fig. 5 for both the wild type and the chlorina mutant. The agreement between the calculated bands and those obtained by numerical deconvolution of the emission spectra is good for the wild type as well as for the chlorina mutant except for the emission associated with the 695 nm absorption form in the wild type. In the emission spectrum of thylakoids from barley wild type there is a small band peaking at about 650 nm which is associated with the Chl *b* absorption band using (Eqn. 1). This emission band is not present in the deconvolution of the emission spectrum of chlorina mutant thylakoids (see Table III).

Discussion

The data presented here show that the room-temperature emission spectra of LHCII and BBY-grana from spinach as well as of thylakoids from barley chlorina mutant and its wild type can be convincingly described as linear combinations of gaussian bands. The number of gaussian components under the major band of the emission spectra corresponds to the number of the absorption spectral forms found in the deconvolution of the Q_y region of the absorption spectra, with a red shift of several nanometres between the emission band series and the absorption band series. For all the preparations investigated similar emission components were found, with the two main bands peaking around 680 nm and 687 nm and several minor bands at shorter and longer wavelengths.

The absorption and emission spectra of a chromophore can be connected using the thermodynamic relation given by Stepanov [18] assuming a thermal relaxation between the vibrational degrees of freedom of the excited chromophore before emission. Using this approach, we have calculated from the absorption bands obtained by numerical deconvolution of the absorption spectra of LHCII, BBY-grana, barley chlorina mutant and its wild type the expected emission bands for a temperature $T = 300$ K. These calculated emission bands are very similar to those found by gaussian deconvolution of the measured emission spectra of the membrane preparations analysed. It therefore seems reasonable to assign an emission band to each of the Chl *a* and Chl *b* absorption bands composing the absorption spectra. The ratio between the area of the fluorescence bands and the corresponding absorption bands is greater for the longer wavelength components than for the shorter ones, giving a clear indication about energy transfer between the different spectral forms. In fact, it is demonstrated that the absorption band population weighted distribution of fluorescence emission may be approximated by the Boltzmann distribution. The correlation between the emission and absorption bands is strong evidence that the different absorption bands obtained by numerical analysis can be interpreted as being due to independent sites of electronic excitation.

The Stokes shifts obtained from our analysis for the different spectral forms range from 2 nm to about 5 nm. Thus it is interesting to note that the wavelength spacing between the maxima of the absorption and emission spectra of chlorophyll containing membranes (about 5–7 nm) does not represent a true Stokes shift. This wavelength spacing is determined not only by the Stokes shifts of the single gaussian components but also by their relative contribution to the emission spectrum. The fact that the overall wavelength difference between the absorption and emission spectra maxima is somewhat greater than the Stokes shift of the single bands is due to the greater contribution made by longer wavelength bands to fluorescence emission than to absorption. Such a result is expected in an energy transferring matrix on the basis of thermodynamic considerations.

In a previous paper [12] the presence of spectral forms with maxima around 684 nm and 695 nm in the absorption spectrum of an LHCII preparation has been reported. We now confirm the presence of both bands in the LHCII absorption spectrum and moreover a correspondence between the 684 nm and 695 nm absorption bands and the emission bands with maximum at 687 nm and 697 nm, respectively, is established. This lends further support to the presence of long-wavelength Chl *a* spectral forms in LHCII, the external antenna of PS II.

The emission spectra examined, with the exclusion of that of thylakoids from the chlorina mutant, have a small emission band associated with Chl *b* absorption (see Figs. 2, 4, 5a). Experimental evidence suggesting a

Chl *b* emission has been previously found by comparing the open trap emission spectrum of the chlorina mutant thylakoids with that of either wild-type barley or isolated LHCII [17]. From this comparison it has been concluded that around 650 nm the Chl *b* emission is roughly equivalent to 2% of the Chl *a* peak value. The contribution of the emission band peaking at 653 nm to the major emission band is around this value (see Table I) and is very similar to the contribution obtained considering a Boltzmann weighted distribution of the excited states of the different chlorophyll forms (Table II).

It is interesting to note that the use of the Stepanov relation to formally calculate the absorption spectrum of LHCII from its total emission spectrum gives an absorption spectrum which is rather similar to the measured one and in which the Chl *b* absorption peak is present (Fig. 3). This peak is, however, not present when the absorption spectrum is calculated from the emission spectrum to which the 653 nm band has been subtracted. This lends further support to the interpretation that the band peaking at about 653 nm in the LHCII emission spectrum is due to a Chl *b* emission.

On the basis of the data presented here it is suggested that each of the different chlorophyll absorption spectral forms has its own separate emission. In the case of the minor Chl *b* emission it has been possible to confirm this interpretation using mutant chloroplasts lacking this component and the Stepanov analysis of the entire emission and absorption bands.

References

1 Thornber, J.P. (1986) in Enc. Plant Physiol. N.S. 19, 98–142.
2 Anderson, J.M. (1986) FEBS Lett. 117, 327–331.
3 Anderson, J.M. (1986) Annu. Rev. Plant Physiol. 37, 93–136.
4 Glazer, A.N. and Melis, A. (1987) Annu. Rev. Plant Physiol. 38, 11–45.
5 French, C.S., Brown, J.S. and Lawrence, M.C. (1972) Plant Physiol. 49, 421–429.
6 Lutz, M. (1977) Biochim. Biophys. Acta 460, 408–430.
7 Butler, W.L. and Hopkins, D.W. (1970) Photochem. Photobiol. 12, 439–450.
8 Brown, J.S. and Schoch, S. (1981) Biochim. Biophys. Acta 636, 201–209.
9 Brown, J.S., Anderson, J.M. and Grimme, L. (1982) Photosynth. Res. 3, 279–291.
10 Brown, J.S. and Schoch, S. (1982) Photosynth. Res. 3, 19–30.
11 Van Dorssen, R.J., Plijter, J.J., Dekker, J.P., Den Ouden, A., Amesz, J. and Van Gorkom, H.J. (1987) Biochim. Biophys. Acta 890, 134–143.
12 Zucchelli, G., Jennings, R.C. and Garlaschi, F.M. (1990) J. Photochem. Photobiol., B: Biol. 6, 381–394.
13 Strasser, R.J. and Butler, W.L. (1977) Biochim. Biophys. Acta 462, 307–313.
14 Rijgersberg, C.P., Amesz, J., Thielen, A.A.G.M. and Swager, J.A. (1979) Biochim. Biophys. Acta 545, 473–482.
15 Marchiarullo, M.A. and Ross, R.T. (1985) Biochim. Biophys. Acta 807, 52–63.
16 Jennings, R.C., Zucchelli, G. and Garlaschi, F.M. (1990) Biochim. Biophys. Acta 1016, 259–265.
17 Jennings, R.C., Zucchelli, G. and Garlaschi, F.M. (1991) Biochim. Biophys. Acta 1060, 245–250.
18 Stepanov, B.I. (1957) Sov. Phys. Dokl. 2, 81–84.
19 Ketskemety, I., Dombi, J. and Horvai, R. (1961) Ann. Physik 8, 342–352.
20 Moss, T.S. (1959) in Optical Properties of Semiconductors, Academic Press, New York.
21 Ryrie, I.J., Anderson, J.M. and Goodchild, D.J. (1980) Eur. J. Biochem. 107, 345–354.
22 Arnon, D.I. (1949) Plant Physiol. 24, 1–15.
23 Ide, J.P., Klug, D.R., Kühlbrandt, W., Giorgi, L.B. and Porter, G. (1987) Biochim. Biophys. Acta 893, 349–364.
24 Berthold, D.A., Babcock, G.T. and Yocum, C.F. (1981) FEBS Lett. 134, 231–234.
25 Zucchelli, G., Garlaschi, F.M. and Jennings, R.C. (1988) Biochim. Biophys. Acta 934, 144–150.
26 Shibata, K. (1958) J. Biochem. (Tokyo) 45, 599–623.
27 Bevington, P.R. (1969) Data Reduction and Error Analysis for the Physical Sciences, McGraw-Hill, New York